STUDY ON THE FLOW STRUCTURES OF THE SHOCKWAVE AND TURBULENT BOUNDARY-LAYER INTERACTION

Wang Bo*, Liu Weidong and Zhao Yuxin**
College of Aerospace and Materials Engineering, National University of Defense Technology
wbsmart_flow@126.com; LWD_INSA@sohu.com.

Keywords: *turbulence, boundary layer, shock wave, separation*

Abstract

The flow organizations of SWBLI field with and without separation were investigated by the high spatiotemporal nanoparticle-based planar laser scattering (NPLS) technique and supersonic particle image velocimetry (PIV). The instantaneous flow field information containing local density, velocity and eddy structures were well presented. In the separated SWBLI field, boundary layer is seen to be distorted seriously, corresponding with complex unsteady shock system. In contrast, no obvious distortion occurs in the unseparated case, and only a strong reflected shock is created. The highly instantaneous three-dimensional flow organization is revealed in the separated SWBLI field. It seems that the detailed eddy structures in an individual NPLS give little evidence on the high- and low- speed streaks inner the incoming boundary layer although they really exist, and their influence on the reverse flow distribution of SWBLI field is well presented both by the NPLS and PIV results. The obvious decrease in the scale of the turbulent eddies could also be observed in the interaction region.

1 Introduction

As a ubiquitous phenomenon encountered in high speed flight, Shock wave and boundary layer interactions (SWBLIs) usually present very complex spatial characteristics and dynamic behaviors, both for external and internal aerodynamics [1]. The relevant studies have been conducted for about sixty years, for its fundamental and practical importance. It may trigger unsteady separation and induce complex fluctuations of aerodynamic and thermal loads, causing fatigue or structural damages, and in all cases downgrading the efficiency of the aircraft or propulsion system [2]. Especially, the shock induced large-scale unsteady separation in the hypersonic/supersonic inlet has become one of the critical problems serious depressing the performance of the scramjet or even leading to inlet unstart [3]. To develop the high efficiency flow control techniques on SWBLIs, a more comprehensive understanding on the foundational physics is of very importance.

Recently, most of the foundational studies on SWBLIs have been focused on the quasi-two dimensional case, incident shock/boundary-layer interaction and flow over a compression ramp. One of the major characteristics of the SWBLI is the unsteady motion of shock system. Such unsteadiness can occur at high frequencies when associated with turbulent fluctuations and to a lesser extent with separated bubble instabilities [4], while a very low frequency fluctuating motion (with order of $O(10\delta/U_\infty)$ to $O(100\delta/U_\infty)$) involving the whole separated region and shock wave system has also been well recognized. However, the origin of this low-frequency movement is still an open question. In the recent years, massive studies on this issue have given us a deeper insight into the physics governing the unsteadiness of the shock. It seems that several mechanisms could contribute to this, including the influence of upstream, downstream conditions and intrinsic shock low-pass filter behavior [5]. The studies focused on the state of incoming boundary layer and the three-dimensional instantaneous flow organizations of SWBLI field [6-9] found that

the spanwise strips of elongated regions of uniform momentum (even with length more than 30δ) in the supersonic incoming boundary layer could obviously affect the instantaneous reflected shock wave and reverse flow pattern, and this could contribute to the low-frequency unsteadiness of the separation region/shock foot in the SWBLI. Some other evidence of a statistical link between low-frequency shock movements and the downstream interaction is also obtained [10-12]. DNS study of Pirozzoli and Grasso [11] indicates that the interaction of coherent structures with the incident shock could produce acoustic waves that propagate upstream and induce an oscillatory motion of the separation bubble, as well as a subsequent flapping motion of the reflected shock wave. Based on the properties of fluid entrainment in the mixing layer generated downstream of the separation shock, Piponniau [12] got a model relating the low-frequency motions to a successive contractions and dilatations of the separated bubble. However, some recently studies also indicated that the interaction unsteadiness would have been induced by SWBLI itself [2,13-17]. The coupling between the shock and boundary layer is found to be mathematically equivalent to a first-order low-pass filter, and the low-frequency unsteadiness in such interactions would be an intrinsic property of the coupled system of the shock and the boundary layer [14,15].

It could be noticed that most conceptions on the unsteadiness of SWBLI mentioned above has been achieved by considering the instantaneous flow organization of separated SWBLI fields, from the innovative experimental studies or high-resolution numerical simulations (LES or DNS). So, the detailed detection and description of the instantaneous flow organization is of very importance. Except for the large-scale movement, another important outcome of interactions of shock waves with turbulent boundary layer is the amplification of velocity fluctuations and substantial changes in length scales. Turbulence amplification through shock wave interactions is considered to be a direct effect of the Rankine-Hugoniot relations. However, there is no agreement among various researchers on how shock interactions affect the length scales, even for the homogeneous turbulence [18].

In the present studies, the instantaneous flow organizations of SWBLI field with and without separation are investigated, while the separated case is paid special attention. The nanoparticle-based planar laser-scattering (NPLS) technique [19-21] used here has the ability to capture high spatiotemporal resolution images of shock waves and turbulent eddy structures in the supersonic flow, which could give more direct insights into the instantaneous flow organization of SWBLI field, and promote the foundational physics studies.

2 Experimental Setup and Technique

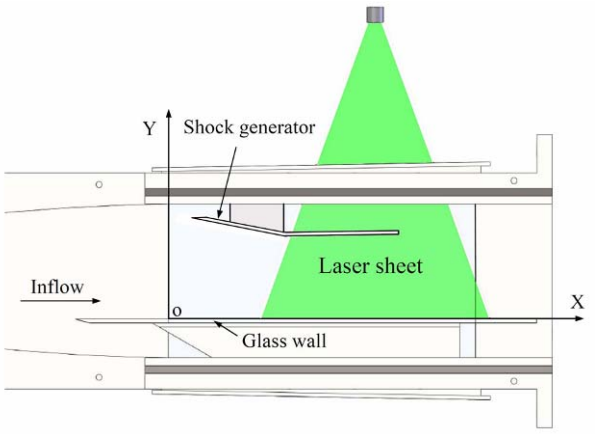

Fig.2.1 Schematic Representation of the Installation.

The experiments have been performed in a Mach 2.7 low-noise wind-tunnel, operating at a stagnation pressure $P_0 = 1.0\times10^5$ Nm^{-2} and stagnation temperature $T_0 = 300K$, with a unit Reynolds number $R_{el} = 8.8\times10^6$ correspondingly. The wind tunnel has a test section of dimensions $200\times200\times400mm^3$ (width × height × Length), giving enough space for the installment of experimental devices, as well as the optical measurements. It is expected that the large spanwise scale could provide a considerable quasi-two dimensional flow field near the median plane of the wind tunnel. The boundary involved experiments are all conducted on the surface of a glass plane (with sharp leading edge) fixed in the main flow of the tunnel (shown in

fig.1). The remarkable benefit is that it could provide a controllable incoming boundary layer state, linear, transitional or turbulent. To get a fully developed turbulent boundary layer, the glass plane has been extended into the nozzle for about 110mm, making sure the boundary layer has an enough developing process. Additionally, a transition bands were implanted on the fore part of the plane to trigger the transition.

Two full-span shock generators, with flow deflection angles of $\alpha = 8^{\circ}$ and 10.5° respectively, are installed on the upper surface of the wind tunnel. The leading edge is kept away from the upper boundary layer to eliminate the possible disturbances (as shown in Fig.2.1). A piece of glass with a 100 mm width is inserted in each steel shock generator to allow passage of a laser sheet and image recording by a CCD camera through the top window. The purpose of this design is to alleviate the influence of the expression wave (originating from the end of the shock generator, unsteady for the separation occurring there) on the flow downstream of SWBLI field, while we could only guarantee the expression wave do not incident directly upon the SWBLI region.

The NPLS [19,20] used here is a Rayleigh-Scattering based flow visualization method, which benefits a lot from the recent development of the nanotechnology, laser and control technique. The fidelity of the tracer particles is expected to be guaranteed by the adoption of nanoparticles, while more intensive signal could also be produced comparing to the molecule-based scattering. In the present study, the seeded flow was illuminated by a PIV-350 double-pulsed Nd:Yag laser, with a 200 mJ pulsed energy and 6ns pulse duration at wavelength 532 nm. The images were recorded by an IMPERX CCD camera with a 4000x2672 pixel sized sensor. The NPLS shears the same equipments with the PIV, so it could be very convenience to carry out the relative experiments simultaneously. The luminance in the NPLS image could reflect the particle distribution, which is mainly attributed to the local fluid density while the particles have been seeded uniformly. However, it is also observed that some other secondary factors would have influenced the distribution of nanoparticles in turbulence field, which would induce some error for presenting the local density but may bring in more benefit for exhibiting the eddy structures of the wall-bounded turbulence [21].

3 Results and Discussion

3.1 Incoming Boundary Layer

High spatiotemporal flow visualization image of the fully developed turbulent boundary layer was captured by NPLS on the streamwise plane, as shown in Fig.3.1 (Detailed flow structures on the spanwise locating 1.5mm above the wall is also presented in the following discussions, Fig.3.4). The dark region has exhibited the detailed structures throughout the entire turbulent boundary layer while the uniform region above it shows the uniform irritation main flow. The time average velocity profile (obtained form PIV measurement) suggests the boundary layer has a thickness of $\delta_{0.99} = 6.3mm$ and an incompressible boundary factor $H_r = \delta^* / \theta \approx 1.4$.

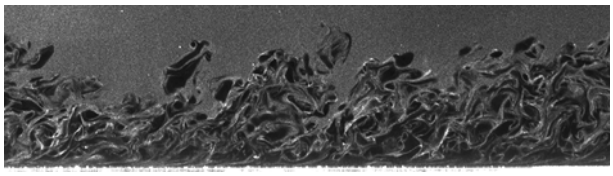

Fig.3.1 Streamwise Flow Structures of the Incoming Turbulent Boundary Layer.

The image indicates that the boundary layer is full of turbulent eddies, while the lifting off of the quasi-streamwise vortexes could be well distinguished close to the wall. The eddy structures presented here has reminded us about the high-resolution direct mumerical simulation (DNS) work of Kaneda & Ishihara [22] who found that the small-scale eddy structures in a homogeneous turbulence are distinctively different from large-scale ones. This means the similarity between different turbulent scales would be doubtful. The interpretation given out by Sagaut [23] is that the 'Richardson cascade' process is only a conception in Fourier space, but not in physical space, and the small scales of the turbulence in the physical space could be

defined as scales associated with gradient of the velocity field. So, it is possible that the images captured by NPLS here have actually been fine enough to present the overall vortex structures inner the boundary.

3.2 Streamwise flow structures of SWBLI field

To begin our investigation on the SWBLI, both of the instantaneous SWBLI fields with and without separation were captured on the streamwise plane, as shown in Fig.3.2 and Fig.3.3 respectively. Even at first glance, remarkable difference features for the two cases could be observed. Under the effect of weaker incident shock (Fig. 3.2, $\alpha = 8^{\circ}$,with shock angle of $\beta = 28.2^{\circ}$), a single strong reflected shock appears, while no obvious distortion of the turbulent boundary layer is presented. This is a typical scene of unseparated SWBLI field, in which the boundary layer has enough momentum to resist the retardation imported by the shock induced adverse pressure gradient. It usually appears a relatively steady state, and does not depart far from the purely inviscid shock reflection solution. It is interesting to observed that the scale of turbulent eddies seems to obviously decreased in the boundary layer downstream of the interaction region.

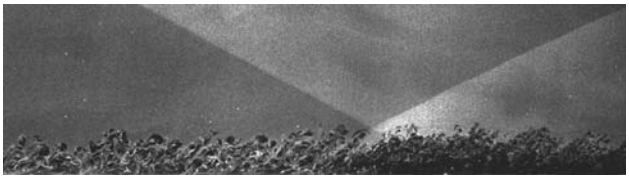

Fig.3.2 Shock Wave and Boundary Layer Interaction Without Separation. (M=2.7, $\alpha = 8^{\circ}$ $\beta = 28.2^{\circ}$)

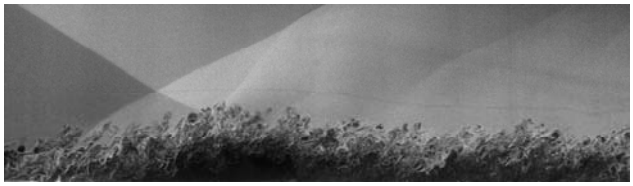

Fig.3.3 Shock Wave and Boundary Layer Interaction With Separation. (M=2.7, $\alpha = 10.5^{\circ}$, $\beta = 30.2^{\circ}$)

As to the separated case, NPLS also gives out a vivid slice of the detailed instantaneous flow structures around the SWBLI field (Fig. 3.3, $\alpha = 10.5^{\circ}$, with shock angle of $\beta = 32.0^{\circ}$). The incidence shock, reflect shock and slip line are all captured, as while as the coherent structures in the boundary layer. The boundary layer is seen to be seriously distorted, with an obvious reverse flow region existing near the wall (see the time averaged PIV results in reference[21]), corresponding with a complex shock system. It is pointed out by Delery [4] that the shock induced entropy production in the interaction with separation would be smaller than in a non-separated interaction, or in the limiting case of the inviscid model. Previous study by Humble [24] suggests that the interaction instantaneously exhibits a multi-layered structure, with a thin region with high shear (or large velocity gradient) originating from the bottom of the incoming boundary layer dividing the interaction region into a high-speed outer region and a low-speed inner region. As we mentioned above, highly unsteadiness feature is observed in the flow field. The separation shock would move up- and down-stream with a range of δ in streamwise, while the second reflect shock would have a much larger fluctuation. The decrease of the turbulent eddy scales is also observed here, and we will have a closer view in the following discussions.

3.3 Spanwise Flow Structures for Separated SWBLI Field

The instantaneous spanwise flow structures of the SWBLI field were also obtained in the experiments. A slice captured on the planes paralleling to the wall (1.5mm or 24% δ above the wall) is shown in Fig.3.4a, with a magnification of partial zone presented in Fig.3.5a. Using the PIV arithmetic (cross-correlation arithmetic), the velocity field is calculated from Fig.3.4a and its counterpart image with a delay of 0.7 μs . So, the instantaneous flow field information containing local density (luminance in NPLS image), velocity and eddy structures are all presented here. This enables us to analyze the flow field from different aspects simultaneously. The dashed line I in Fig.3.4a approximately denotes the reflected shock location while the line II denotes the start of separation.

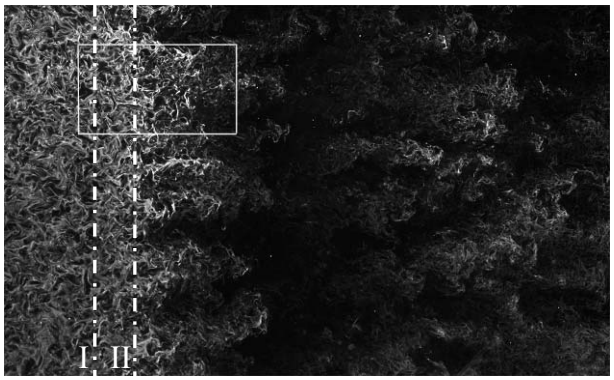

Fig.3.4a Instantaneous Spanwise Flow Organization of Separated SWBLI Field, 1.5mm（or 24%δ）above the Wall.

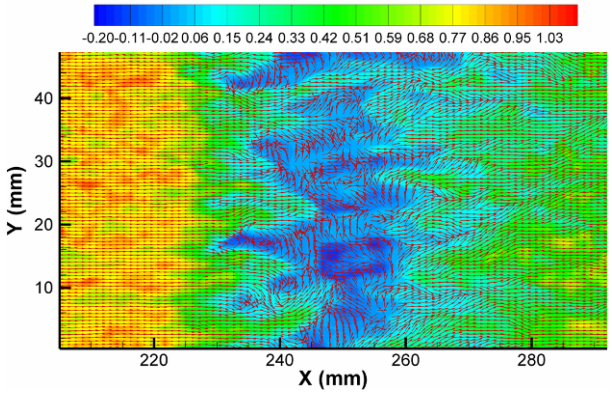

Fig.3.4b Instantaneous Streamwise Velocity Distribution on the Spanwise, Calculating with PIV Arithmetic from Fig.3.4a. Vector is Added to Denote the Flow Direction.

Different from the observation of Ganapathisubramani [7] with condensed acetone fog based planar laser scattering, no evidence of the very large-scale streaks (more than 30δ) in the incoming boundary layer is observed from the present flow visualization, except the much more detailed vortex structures as shown in Fig.3.4a and Fig.3.5. This does not mean there are no speed streaks. Actually, we could just observe them in the velocity field corresponding to the NPLS image. Considering the fact that the luminance presents in the NPLS image is mainly influence by the local density (with some error on the verge of the eddies), we could presume that the speed streaks in the boundary layer have no obvious effect on the density field, and they have been hidden in the turbulence background in Fig.3.4a. This means the eddy structure observed in an individual NPLS image carries very limited local velocity information. So, these eddy structures and their scale observed here would be different from the velocity based statistical result.

Comparing with the velocity field shown in Fig.3.4b, it is easy to found that the regions with low luminance present in Fig.3.4a have actually indicated the strong reverse fluid inner the SWBLI field. This could be induced by the high temperature and low density feature of the stagnation or reverse flow. Fig.3.4 -a and -b suggest the instantaneous SWBLI field has highly three-dimensional organization forms, with some spanwise reverse flow streaks inserting into the positive flow in the start of the interaction region. As described by Humble [9] and Ganapathisubramani [7], the local momentum distribution would have influences the ability of the fluid to resist the separation, making the separation line exhibits large-scale undulations conforming to the low- and high-speed streaks beneath the incoming boundary layer. Further to the description, it is found in the present study that the effect of the speed streaks could promulgate further downstream, influencing the whole separation region and producing some other elongated reverse or low speed flow streaks near the reattached region. Additionally, it has been commonly considered that the mass flow in the separated region is supplied by the flow coming from the downstream. However, velocity direction in Fig.3.4b indicates that the reverse flow could also be supplied by the positive flow. Thus, the fluid and energy transportation on the spanwise would be an important feature for the separated SWBLI field.

Another notable phenomenon is the decrease of the turbulent eddy scales in the interaction region. A partial zone marked in Fig.3.4a is exhibited in Fig.3.5a, in which the turbulent eddies inner the incoming boundary layer is well presented. While the flow enters into the interaction region, the local density decreases obviously, corresponding with changing of the discernable turbulence eddy scale. This may be in accordance with the general opinion that the fluctuations are amplified with length scales decreased across the shock wave. However, we could see from the streamwise flow structures (Fig.3.5b) that

the boundary fluid ascending along the shear layer upon the separated flow may have no such obvious change. This means the scale changes would meanly happened for the stagnation or reverse flow beneath the shear layer of the separated SWBLI field.

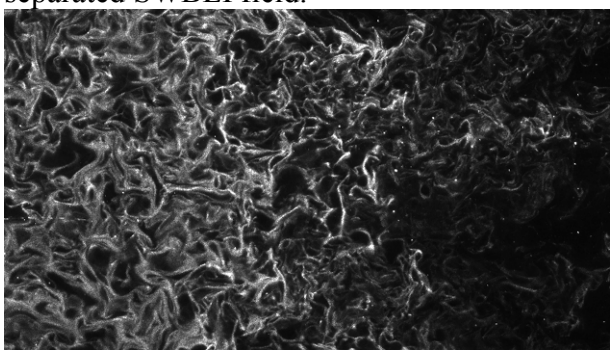

Fig.3.5a Decrease of Turbulent Scales, Emphasis of a Partial Zone as Marked in Fig.3.4a.

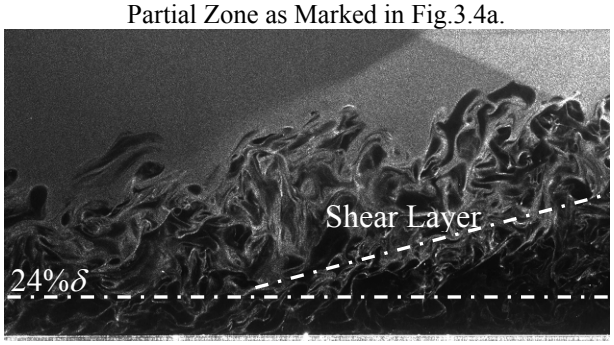

Fig.5.b Magnified flow structure on the streamwise near the reflected shock foot.

4 Conclusion

To have a further understanding on the foundational physics underlaying the shock wave and turbulent boundary layer interaction (SWBLI), the instantaneous flow fields were invested with the nanoparticle-based planar laser-scattering. The high spatiotemporal flow structures in wall-bounded turbulence and SWBLI fields (both for the unseparated and separated cases) were well captured. It seems that turbulent eddies with different scales (streamwise and spanwise) exhibit no spatial structural similarity, as suggested by the study of Kaneda & Ishihara and Priebe [22,17] in homogeneous turbulence.

In the weak SWBLI field where no obvious distortion of boundary layer occurs, only a strong reflected shock is created, similar to the inviscid model. For the strong interaction case, the boundary layer has been seriously distorted, with an obvious reverse flow region existing near the wall, corresponding with a complex shock system. The instantaneous flow structures containing information of local density, velocity and eddy forms were presented. Especially, a slice captured on the spanwise plane1.5mm above the wall reveals a highly three-dimensional instantaneous flow organization form of separated SWBLI field, with some separated streaks inserting into the positive flow in the start of the interaction region, which would have been induced by the velocity streaks in the incoming boundary layer. This spanwise structure has influence on the whole separated flow field, inducing formation of reverse flow streaks near reattached region and transportation of fluid on the spanwise. The obvious decrease in the scale of turbulent eddies have also been observed in the interaction region.

References

[1] Dolling D S. 50 years of shock wave/boundary layer interaction-what next? AIAA Paper 2000-2596, 2000.

[2] Doerffer P, Hirsch C, Dussauge J P, Babinsky H and Barakos G N. Unsteady Effects of Shock Wave Induced Separation. Springer, 2010.

[3] Babinsky H and Ogawa H. SBLI control for wings and inlets. Shock Waves, Vol.18, pp 89-96, 2008.

[4] Délery J and Dussauge J P. Some physical aspects of shock wave/boundary layer interactions. Shock Waves, Vol.19, pp 453-468, 2009.

[5] Dussauge J P and Piponniau S. Shock/boundary-layer interactions: Possible sources of unsteadiness. Journal of Fluids and Structures. Vol. 24, pp 1166-1175, 2008.

[6] Beresh S J, Clemens N T and Dolling D S. Relationship between upstream turbulent boundary layer velocity fluctuations and separation shock unsteadiness. AIAA Journal. Vol.40, No.12, pp 2412-2422, 2002.

[7] Ganapathisubramani B, Clemens N T, and Dolling D S. Effects of upstream boundary layer on the unsteadiness of shock-induced separation. Journal of Fluid Mechanism. Vol.585, pp 369-394, 2007.

[8] Ganapathisubramani B, Clemens N T, and Dolling D S. Low-frequency dynamics of shock-induced separation in a compression ramp interaction. Journal of Fluid Mechanism. Vol.636, pp 397-425, 2009.

[9] Humbler R A, Elsinga G E, Scrano F and van Oudheusden B.W. Three-dimensional instantaneous structure of a shock wave/turbulent boundary layer interaction. Journal of Fluid Mechanism. Vol.622, pp 33-62, 2009.

[10] Dupont P, Haddad C. and Debieve J F. Space and time organization in a shock-induced separated boundary layer. Journal of Fluid Mechanism, vol.559, pp 255-277, 2006

[11] Pirozzolia S and Grasso F. Direct numerical simulation of impinging shock wave/turbulent boundary layer interaction at M=2.25. PHYSICS OF FLUIDS, Vol.18, 065113, 2006

[12] PIPONNIAU S, DUS SAUGE J P, DEBIEVE J F and DUPONT P. A simple model for low-frequency unsteadiness in shock-induced separation. Journal of Fluid Mechanism, vol. 629, pp 87-108,2009

[13] Touber E and Sandham N D. Comparison of three large-eddy simulations of shock-induced turbulent separation bubbles. Shock Waves. Vol.19, pp 469-478, 2009.

[14] Touber E and Sandham N D. Low-order stochastic modelling of low-frequency motions in reflected shock-wave/boundary-layer interactions. Journal of Fluid Mechanism, Vol. 671, pp 417-465, 2011.

[15] Plotkin, K. J. Shock wave oscillation driven by turbulent boundary-layer fluctuations. AIAA Journal, Vol.13, Nol. 8, pp 1036-1040, 1975.

[16] Li X L, Fu D X, Ma Y W and Liang X. Direct numerical simulation of shock/turbulent boundary layer interaction in a supersonic compression ramp. SCIENCE CHINA Physics, Mechanics & Astronomy. Vol.53, No.9, pp 1651-1658, 2010

[17] Priebe S and Martín M P. Low-frequency unsteadiness in shock wave_turbulent boundary layer interaction. Journal of Fluid Mechanism, vol.699, pp 1-49, 2012.

[18] Andreopoulos Y, Agui J H, and Briassulis G, SHOCK WAVE–TURBULENCE INTERACTIONS, Annu. Rev. Fluid Mech. Vol.32, pp 309-345, 2000.

[19] Yi S H, He L, Zhao Y X, Tian L F, and Cheng Z Y. A flow control study of a supersonic mixing layer via NPLS. Sci. China Ser. G, Vol.52. No.12, pp 2001-2006, 2009.

[20] Zhao Y X, Yi S H, He L, and Cheng Z Y. Supersonic flow imaging via nanoparticles. Sci. China Ser. E: Technol. Sci, Vol.52, No.12, pp 3640-3648, 2009.

[21] Wang B, Liu W D, Zhao Y X, Fan X Q, and Wang C. Experimental investigation of the micro-ramp based shock wave and turbulent boundary layer interaction control. PHYSICS OF FLUIDS. Vol.24, 055110, 2012.

[22] Kaneda Y and Ishihara T. High-resolution direct numerical simulation of turbulence. Journal of Turbulence. Vol7, No. 20, pp:1-17, 2006

[23] Sagaut P. Homogeneous Turbulence Dynamics. Cambridge University Press. 2008.

[24] Humble R A, Scarano F, and Oudheusden B W V. Particle image velocimetrymeasurements of a shockwave/turbulent boundary layer interaction. Exp. Fluids, Vol. 43, pp173-183, 2007.

Copyright Statement